

Full title: Investigating the Substrate Specificity of the Neutral Sphingomyelinase
from *Trypanosoma brucei*

Emily A. Dickie¹, Simon A. Young and Terry K. Smith

Biomedical Sciences Research Complex, Schools of Biology and Chemistry,
University of St Andrews, Fife, KY16 9ST, UK

Running title: *T. brucei* neutral sphingomyelinase substrate specificity

Correspondence should be addressed to Terry K. Smith. Address: Biomedical Sciences
Research Complex, Schools of Biology and Chemistry, University of St Andrews, Fife,
KY16 9ST, UK. Telephone: +44(0)1334 463412. Email: tks1@st-andrews.ac.uk

¹ Current address: Wellcome Trust Centre for Molecular Parasitology, Institute of Infection,
Immunity and Inflammation, College of Medical, Veterinary and Life Sciences, University of
Glasgow, Glasgow, G12 8TA, UK

16 ABSTRACT

17 The kinetoplastid parasite *Trypanosoma brucei* causes African trypanosomiasis in both
18 humans and animals. Infections place a significant health and economic burden on
19 developing nations in sub-Saharan Africa, but few effective anti-parasitic treatments are
20 currently available. Hence, there is an urgent need to identify new leads for drug
21 development. The *T. brucei* neutral sphingomyelinase (TbnSMase) was previously
22 established as essential to parasite survival, consequently being identified as a potential drug
23 target. This enzyme may catalyse the single route to sphingolipid catabolism outside the
24 *T. brucei* lysosome. To obtain new insight into parasite sphingolipid catabolism, the substrate
25 specificity of TbnSMase was investigated using electrospray ionization tandem mass
26 spectrometry (ESI-MS/MS). TbnSMase was shown to degrade sphingomyelin,
27 inositol-phosphoceramide and ethanolamine-phosphoceramide sphingolipid substrates,
28 consistent with the sphingolipid complement of the parasites. TbnSMase also catabolised
29 ceramide-1-phosphate, but was inactive towards sphingosine-1-phosphate. The broad-range
30 specificity of this enzyme towards sphingolipid species is a unique feature of TbnSMase.
31 Additionally, ESI-MS/MS analysis revealed previously uncharacterised activity towards
32 *lyso*-phosphatidylcholine (*lyso*-PC), despite the enzyme's inability to degrade PC.
33 Collectively, these data underline the enzyme's importance in choline homeostasis and the
34 turnover of sphingolipids in *T. brucei*.

35 **KEYWORDS:** lipid catabolism, sphingolipid, choline, lipid extraction, mass spectrometry,
36 enzyme, activity assay

37

38 **KEY FINDINGS**

- 39 • TbnSMase has broad substrate specificity towards various sphingolipids
- 40 • TbnSMase is the first *T. brucei* enzyme shown to catabolise lyso-phosphatidylcholine
- 41 • Sphingosine-1-phosphate, glycosphingolipids and phosphatidylcholine are not
- 42 TbnSMase substrates
- 43 • TbnSMase plays a direct role in choline homeostasis in bloodstream form parasites

44 **INTRODUCTION**

45 The kinetoplastid parasite *Trypanosoma brucei* causes African trypanosomiasis in both

46 humans and animals. Human African trypanosomiasis (HAT) is considered fatal if left

47 untreated, and poses a serious health risk to an estimated 65 million people in Sub-Saharan

48 Africa (World Health Organization, 2017a). Recent efforts have led to a dramatic decrease in

49 reported disease cases, with 2804 cases reported in 2015, although the World Health

50 Organization estimates the actual number of cases to be 10-fold greater (World Health

51 Organization, 2017a; b). Research has also produced promising new drug candidates,

52 however, the risk of parasite resistance and consequent HAT re-emergence still threaten the

53 progress made in combatting the disease. Animal trypanosomiasis remains a significant

54 burden, with billions of US dollars lost through livestock infections each year and few

55 treatment candidates on the horizon (Shaw *et al.*, 2014). Thus, there is an urgent need to

56 identify leads for drug development.

57 *T. brucei* sphingolipid biosynthesis has long been identified as a potential drug target. Most

58 eukaryotes are capable of synthesising their own sphingolipids via the *de novo* biosynthesis

59 pathway (**Fig. 1A**), which is highly conserved amongst eukaryotic organisms (Kolter and

60 Sandhoff, 1999). Although homologues of most of the enzymes involved in this biosynthetic

61 pathway have been (putatively) identified in *T. brucei*, many still require biochemical

62 characterisation (Smith and Bütikofer, 2010). The first reaction in the pathway, condensation

63 of serine and palmitoyl-CoA, is catalysed by the enzyme serine-palmitoyltransferase (SPT)

64 (Tidhar and Futerman, 2013). A homologue of this enzyme has been identified in *T. brucei*,

65 which was shown to be essential for cell cycle progression and parasite survival (Fridberg *et al.*

66 *et al.*, 2008). Inhibiting the initial SPT-catalysed reaction of the *T. brucei* *de novo* biosynthesis

67 pathway disrupted procyclic cytokinesis and kinetoplast segregation, validating the pathway

68 as a drug target (Fridberg *et al.*, 2008; Smith and Bütikofer, 2010). Although SPT is known to

69 be essential in other parasites, such as *Plasmodium falciparum* (Gerold and Schwarz, 2001),
70 these findings contrast with research involving the related kinetoplastid parasite *Leishmania*
71 *major* (Denny *et al.*, 2004; Zhang *et al.*, 2007). Unusually, *T. brucei* has four tandemly linked
72 genes, each encoding different sphingolipid synthases (TbSLSs1-4) (Sevova *et al.*, 2010).
73 This family of sphingolipid synthases is orthologous to the *S. cerevisiae* *AURI*-encoded IPC
74 synthase (Mina *et al.*, 2009), and equivalent enzymes are found in both *Leishmania major*
75 (Denny *et al.*, 2006) and *Trypanosoma cruzi* (De Lederkremer *et al.*, 2011). RNA
76 interference (RNAi) against the *TbSLSI-4* gene locus in bloodstream trypanosomes impeded
77 growth, ultimately leading to parasite death (Sutterwala *et al.*, 2008). This finding identified
78 the TbSLSs as potential drug targets. The individual functional specificities of the four
79 synthases were determined by employing a cell-free synthesis system (Sevova *et al.*, 2010).
80 TbSLSs 1 and 2 synthesise IPC and EPC respectively (Sevova *et al.*, 2010). TbSLSs 3 and 4
81 are bi-functional, producing both SM and EPC (Sevova *et al.*, 2010). Research has indicated
82 TbSLS substrate specificity is dictated by natural variations in a small number of active site
83 residues, thought to be involved in acid-base catalysis (Goren *et al.*, 2011). Establishing the
84 functions of the TbSLSs has clarified how the parasite is capable of altering its sphingolipid
85 complement during its life cycle (Mina *et al.*, 2009; Sevova *et al.*, 2010), an observation
86 further confirmed by recent sphingolipidomic analysis (Guan and Mäser, 2017). Currently,
87 trypanosomatids are the only organisms known to synthesise sphingolipid species with
88 choline, ethanolamine and inositol headgroups (Serricchio and Bütikofer, 2011; Guan and
89 Mäser, 2017).

90 In comparison to the knowledge of *T. brucei* sphingolipid biosynthesis that has already been
91 acquired, little is known of the processes involved in the parasites' sphingolipid catabolism.
92 The catabolism of sphingolipids in eukaryotes takes place via the degradation pathway
93 (**Fig. 1B**), predominantly in lysosomes and late endosomes, but also in other cellular
94 locations (Kolter and Sandhoff, 1999; Jenkins *et al.*, 2009). A number of different enzymes
95 are involved in the degradative process (ceramidases, lyases, phospholipase D), but one
96 major group of proteins responsible for sphingolipid turnover in mammalian cells is the
97 sphingomyelinase (SMase) enzyme family (Kolter and Sandhoff, 1999). As indicated by their
98 name, the primary substrate of these enzymes in mammals is SM, which is hydrolysed to
99 yield ceramide and choline-phosphate (ChoP) (Jenkins *et al.*, 2011). *T. brucei* has a single
100 neutral SMase (TbnSMase) (Q57U95), a membrane protein with two identified
101 transmembrane domains at its C-terminus (Young and Smith, 2010). TbnSMase has been

localised to the ER in bloodstream form parasites, and genetically confirmed as a potential drug target (Young and Smith, 2010). The activity of this protein is thought to be essential due to its intrinsic roles in vital biochemical processes, including choline and ceramide homeostasis, and endocytosis. This is particularly relevant to the coupling of endocytic and exocytic mechanisms with post-Golgi sorting of GPI-anchored variant surface glycoprotein (VSG), which is needed to maintain VSG surface density (Young and Smith, 2010). VSG molecules form the protective coat that permits *T. brucei* parasites to evade the host immune system (Mugnier *et al.*, 2016). The importance of TbnSMase corroborates findings relating to the single leishmanial sphingolipid degradative enzyme (ISCL), another nSMase homologue (Zhang *et al.*, 2009; McConville and Naderer, 2011). ISCL IPCase activity is required for *L. major* promastigote stationary phase survival, most noticeably at acidic pH (Xu *et al.*, 2011). The enzyme's SMase function is necessary for amastigote proliferation and virulence in mammalian hosts (Zhang *et al.*, 2009, 2012). This means that the importance of leishmanial ISCL activity is linked to cell cycle stage (Zhang *et al.*, 2012). Similarly, inhibiting the nSMase/lyso-PC phospholipase C of *Plasmodium falciparum* disrupts parasite intra-erythrocytic proliferation, suggesting the protein could serve as a drug target (Hanada *et al.*, 2002). In previous research, TbnSMase was shown to catabolise SM effectively, but was inactive towards phosphatidylcholine (PC) (Young and Smith, 2010). This initial analysis has now been taken forward to provide a more comprehensive overview of TbnSMase lipid degradative activity and specificity.

MATERIALS AND METHODS

Unless otherwise stated, all reagents and materials were purchased from Sigma, Promega, Thermo Scientific or VWR. C-1-P (d18:1/16:0), EPC (d17:1/12:0), SM (brain, porcine), dipalmitoyl-PC and dimyristoyl-PC (used as a mass spectrometry standard) were purchased from Avanti Polar Lipids. SM (D18:1/6:0), lyso-PC (from egg yolk), S-1-P (d18:1), and galactosylceramide were purchased from Sigma. EPC (from buttermilk, semi-synthetic) was purchased from Matreya LLC. Procytic cell culture media were filter sterilised with either Millex GP 0.22 μ M syringe filters or Triple Red 0.22 μ M vacuum filtration units. Parasite cultures were maintained in Greiner Bio-One CELLSTAR® tissue culture flasks.

Recombinant expression of TbnSMase (Q57U95) in *E. coli*

A pGEX-6P-1-TbnSMase expression construct was employed as previously described (Young and Smith, 2010). The expression construct was used to transform BL21 pLysSGold *E. coli*. Positive clones were selected using ampicillin-agar plates ($100 \mu\text{g mL}^{-1}$) supplemented with chloramphenicol ($34 \mu\text{g mL}^{-1}$). Three bacterial colonies were used to inoculate $3 \times 10 \text{ mL}$ of LB media (Miller composition, supplemented with $50 \mu\text{g mL}^{-1}$ ampicillin and $34 \mu\text{g mL}^{-1}$ chloramphenicol). After a 24 hour incubation, the 10 mL overnight cultures were combined in a single tube (30 mL total volume). The combined culture was then used to inoculate $3 \times 1 \text{ L}$ auto-induction (AI) media (Formedium, supplemented with $50 \mu\text{g mL}^{-1}$ ampicillin and $34 \mu\text{g mL}^{-1}$ chloramphenicol), using 10 mL of overnight culture per litre flask of AI media. Cells were grown at 37°C for 4 hours before the temperature was decreased to 25°C for a further 20 -hour incubation. GST-TbnSMase-enriched bacterial membranes were prepared from these cultures. Pellets of 500 mL spun-down culture were washed in PBS and stored at -80°C until they could be processed.

TbnSMase-enriched bacterial membrane preparation

The protocol described is adapted from methods previously outlined (Young and Smith, 2010). Pellets of 500 mL spun-down bacterial culture were suspended and lysed in 10 mL lysis buffer (50 mM Tris.HCl (pH 8.0), 300 mM NaCl, 10% glycerol (v/v), 5 mM MgCl_2 , 1 mM DTT), containing 0.2 mg mL^{-1} lysozyme (Sigma), Merck Millipore Benzonase® Endonuclease ($250 \text{ units mL}^{-1}$ lysate) and 1 x protease inhibitor tablet (Roche). The lysis solution was incubated for 30 minutes at 37°C , followed by probe sonication at 4°C (6 minutes total, 30 seconds on/30 seconds off). The lysate was then centrifuged at $14,500 \times g$, 20 minutes. The product supernatant was divided amongst 3.2 mL capacity Beckman Coulter ultra-centrifuge tubes ($\times 3$) for ultra-centrifugation at $100,000 \times g$, 1 hour. Pellets were washed with 1.5 mL PBS. Bacterial membrane pellets were then suspended in $500 \mu\text{L}$ buffer each (100 mM Tris-HCl (pH 7.4), 10 mM MgCl_2 , 20% glycerol) using a combination of vortexing and water bath sonication (25°C , 4 minutes). The total membrane suspension ($1500 \mu\text{L}$ total volume) was mixed in a single tube and was then aliquoted ($50\text{-}100 \mu\text{L}$). Aliquots were flash-frozen using liquid nitrogen and stored at -80°C . Total protein in each membrane preparation was quantified using the BCA Protein Assay Kit

164 (Thermo Scientific). The presence of TbnSMase in bacterial membranes was confirmed by
165 mass spectrometry.

166 Amplex® UltraRed assay

167 Amplex® UltraRed assay coupling enzyme solutions were prepared from lyophilized
168 powders using dH₂O, and were stored as small aliquots at -20°C. Alkaline phosphatase
169 (AlkPhos) (Sigma) from bovine intestinal mucosa was prepared as a 400 units mL⁻¹ stock
170 solution. Choline oxidase (ChoOx) (Sigma) from *Alcaligenes* sp. was prepared at
171 20 units mL⁻¹, horseradish peroxidase (HRP) (Sigma) at 200 units mL⁻¹. Desiccated aliquots
172 of Amplex® UltraRed reagent (Thermo Scientific) were suspended in 340 µL DMSO, as
173 directed by the manufacturer, and stored at -20°C in small aliquots. To assay the aqueous
174 fractions of biphasically separated GST-TbnSMase SM substrate reactions, aqueous phases
175 were dried using a Savant SPD121P SpeedVac concentrator. The fractions were suspended in
176 100 µL reaction buffer (100 mM HEPES (pH 7.4), 10 mM MgCl₂) and divided between
177 2 wells of a black 96-well reaction plate (50 µL per well). Additional reaction buffer (50 µL)
178 was then added to each well. A mastermix of Amplex® assay components (coupling enzymes
179 and Amplex® UltraRed reagent) was prepared. The mastermix accounted for the addition of
180 2 µL AlkPhos, 1.5 µL ChoOx, 1 µL HRP, 0.25 µL Amplex UltraRed reagent and 95.25 µL
181 reaction buffer per well (total reaction volume per well was 200 µL). Change in fluorescence
182 (Ex. 560 nm, Em. 587 nm) was then monitored for 1 hour using a Spectra Max Gemini XPS
183 fluorescence plate reader at 37°C. Results were recorded using SoftMax Pro v 5.2 software.

184 Lipid substrate activity assays

185 Lipid substrates were suspended in 2% Triton X-100 to the desired stock concentration
186 through vortexing and water-bath sonication (10 minutes). Substrate mass was substrate- and
187 analysis-dependent (20-50 nmoles), but each was added to reactions (50-100 µL total
188 volume) to a final concentration of 0.1-0.2% Triton X-100. Substrates were incubated with
189 TbnSMase-enriched bacterial membranes (~100 µg total protein) in 1.5 mL
190 solvent-resistant microcentrifuge tubes. In heat-inactivated protein reactions, protein aliquots
191 were heated to 95°C (20 minutes) prior to substrate addition. Reactions were performed in
192 100 mM HEPES (pH 7.4), 10 mM MgCl₂ buffer. On substrate addition, reactions were mixed
193 briefly and sonicated for 30 seconds in a water bath (25°C). Reaction tubes were then
194 incubated at 37°C (4 hours) in a water bath. Following incubation, reactions were quenched

with 800 μL CHCl_3 . If required, mass spectrometry standards (e.g. PC 28:0) were then added (500 pmoles), prior to the addition of 250 μL dH_2O . The organic phase was isolated following the Bligh and Dyer biphasic separation method (Bligh and Dyer, 1959), and dried under nitrogen.

Parasite lysate NBD-IPC activity assays

Cells were suspended in lysis buffer (25 mM Tris (pH 7.5), 0.1% Triton X-100, 1 x protease inhibitor tablet (Roche)) to a density of $\geq 2 \times 10^8$ cells mL^{-1} , and were incubated on ice for 5 minutes. Subsequently, 4×10^6 parasites from each stock were transferred to each reaction. Parasites were incubated with 0.8 nmoles NBD-IPC, in 50 mM Tris (pH 7.5), 5 mM MgCl_2 , 5 mM DTT, 0.1 % Triton X-100 reaction buffer, for 1 hour at 25 °C with gentle agitation (protected from the light). Following incubation, reactions were quenched with the addition of 1 mL CHCl_3 . Subsequently, 500 μL MeOH and 200 μL dH_2O were quickly added. Samples were vortex mixed, then left to stand (protected from the light). The organic phase from each sample was isolated through biphasic separation, and dried under nitrogen.

High-performance thin-layer chromatography

HPTLC analysis of EPC and NBD-IPC substrate reactions was conducted using a CHCl_3 : MeOH: dH_2O solvent system (65:25:4). Dried lipid samples were resuspended in 2:1 CHCl_3 : MeOH (10-20 μL volume) and were gradually spotted onto HPTLC plates. EPC reaction results were visualised by treating HPTLC plates with ninhydrin solution (1% w/v in butan-1-ol). NBD-IPC reaction results were visualised via fluorescence imaging using a Typhoon FLA 7000 (GE), with CY2 (filter Y520, 473 nm laser) and Sypro Ruby (filter O580, 473 nm laser) settings.

Procyclic form *T. brucei* lipid extract preparation

T. brucei (Lister 427 (29-13) strain) procyclic (PCF) parasites were grown in SDM-79 media at pH 7.4, as previously described (Brun and Schönenberger, 1979). Drugs G418 ($15 \mu\text{g mL}^{-1}$) and hygromycin ($50 \mu\text{g mL}^{-1}$) were included in the media in order to maintain the expression of a tetracycline repressor and T7 RNA polymerase (Wirtz *et al.*, 1999). A 10 ml culture of PCF cells ($\sim 1 \times 10^7$ cells mL^{-1}) was pelleted via centrifugation at 800 x g, 10 minutes. The cell pellet was resuspended in a minimal volume of media ($\sim 500 \mu\text{L}$) and transferred to a microcentrifuge tube for further centrifugation (3800 x g, 3 minutes). Cells

were washed in 1 mL PBS, and then re-pelleted (3800 x g, 3 minutes). The pellet was resuspended in 200 μ L PBS and transferred to a glass vial containing 750 μ L 2:1 MeOH:CHCl₃ for biphasic separation, based on the method described by Bligh and Dyer (Bligh and Dyer, 1959). The sample was dried under nitrogen and stored at 4°C until use.

Electrospray tandem mass spectrometry

Lipid samples were analysed by electrospray tandem mass spectrometry (ESI-MS/MS) with an AB-Sciex Qtrap 4000 triple quadrupole mass spectrometer, incorporating an Advion TriVersa NanoMate nanoelectrospray ionisation source. Single-stage MS in negative ion mode was used to obtain survey scans of phosphatidylethanolamine (PE), ethanolamine-phosphoceramide (EPC), phosphatidylinositol (PI), inositol-phosphoceramide (IPC) and ceramide (Cer) species (cone voltage = 1.25 kV). Positive ion mode survey scans were used to detect phosphatidylcholine (PC) and sphingomyelin (SM) species (cone voltage = 1.25 kV). In tandem mass spectrometry, nitrogen was the collision gas. To examine PC/SM species, positive ion mode scans to detect precursors of m/z 184 were performed, with 50 eV collision energy (CE). In negative ion mode, precursors of m/z 196 scans allowed the identification of PE and EPC lipids, precursors of m/z 241 scans were used to observe PI and IPC species (CE = 60). Spectra were acquired over or within the range of 120-1000 m/z, and each spectrum represents a minimum of 30 consecutive scans. Samples were run using a 1:1 solvent mixture of 2:1 MeOH: CHCl₃ and 6:7:2 acetonitrile: isopropanol: dH₂O.

RESULTS

GST-TbnSMase was recombinantly expressed in *E. coli* to produce TbnSMase-enriched bacterial membranes, using previously described methods (Young and Smith, 2010). The presence of the GST-TbnSMase membrane protein was confirmed using mass spectrometry (**Fig. S1**). After isolating the bacterial membranes via ultra-centrifugation, it was possible to assay GST-TbnSMase activity directly from the membranes with minimal bacteria-derived background activity, removing the need for protein purification. This had also been achieved during previous research into TbnSMase activity (Young and Smith, 2010). To confirm the GST-TbnSMase recombinant protein was active, GST-TbnSMase-enriched bacterial membranes were first incubated at 37 °C for 4 hours with a sphingomyelin (SM) substrate. The substrate used was Avanti Polar Lipids brain SM (product no. 860062). Although this

product is enriched for SM 36:1 (d18:1/18:0), as a natural lipid preparation the product is a mixture of brain SM species. The spectra presented here are consistent with the recently released Avanti Polar Lipids fatty acid distribution analysis for this product (**Fig. S2**) (Avanti Polar Lipids, 2018). Following SM substrate incubation, reactions were biphasically separated using 2:1 CHCl₃: MeOH to isolate the lipid-rich organic phase. ESI-MS/MS was used to detect the levels of choline-containing (SM) lipid species in lipid samples derived from both active GST-TbnSMase and heat-inactivated GST-TbnSMase reactions (**Fig. 2A and 2B, see also Fig. S3**). A dimyristoyl-PC standard was added to each sample during lipid extraction, allowing SM substrate peak intensities to be normalised against the intensity of the internal standard. Relative peak intensities for each SM substrate species are shown (**Fig. 2C**).

The catabolic activity of GST-TbnSMase towards sphingomyelin had been demonstrated previously (Young and Smith, 2010), here providing confirmation that the GST-TbnSMase recombinant protein was active. However, the use of ESI-MS/MS allowed the relative turnover of individual SM species present in the substrate mixture to be compared (**Fig. 2C**). The results indicate that GST-TbnSMase is active towards SM species with a range of fatty acid chain lengths (C16-C24). There was a 2.6-fold (62%) decrease in SM 42:1 (d18:1/24:0)/SM 42:2 (d18:1/24:1), compared to a 1.5-fold (35%) decrease in SM 36:1 (d18:1/18:0), despite the latter lipid being the prevalent species in the SM substrate mixture. This may indicate GST-TbnSMase preferentially degrades sphingolipid species of specific fatty acid chain lengths. SM substrate catabolism was further confirmed by identification of product ceramide chloride adducts $[M + Cl]^-$ in negative ion mode survey scans (**Fig. 3**). Product ceramides were observed in the active GST-TbnSMase reaction (**Fig. 3A**), and were absent from the heat-inactivated control (**Fig. 3B**). Additionally, aqueous fractions isolated during biphasic separation of SM substrate reactions were tested for the presence of choline phosphate. The aqueous fractions were used as substrates for the Amplex® UltraRed assay system. In this assay (**Fig. S4**), the coupling enzyme alkaline phosphatase (AlkPhos) is included to dephosphorylate choline phosphate, yielding choline. The choline produced then serves as a substrate for the second coupling enzyme in the system: choline oxidase (ChoOx). Only the aqueous fractions from the active GST-TbnSMase reactions, in the presence of alkaline phosphatase, induced significantly increased rates of fluorescence change (**Fig. 3C**). These results confirm GST-TbnSMase is a

phosphodiesterase C enzyme, degrading SM substrates to form ceramide and choline phosphate.

Having established the GST-TbnSMase protein was active, the enzyme's activity towards a number of different sphingolipid substrates was examined. As already highlighted, *T. brucei* is known to produce SM, EPC and IPC. Thus, it was important to examine the activity of TbnSMase towards EPC and IPC sphingolipids. Firstly, GST-TbnSMase was incubated with an EPC substrate. The EPC substrate used was supplied by Mattreya LLC (product no. 1327), a semi-synthetic preparation derived from bovine buttermilk. No fatty acid distribution analysis is available for this product. However, the average molecular weight reported for the product (mw = 773) appears consistent with our analysis (**Fig. 4A**). Lipid extracts from the EPC substrate reactions were analysed in ESI-MS/MS negative ion mode survey scans. The EPC species present in the substrate (**Fig. 4A**) were efficiently degraded by GST-TbnSMase, yielding ceramide products (**Fig. 4B**). These products were absent from the heat-inactivated GST-TbnSMase control and the EPC/Triton X-100 detergent mixed micelles supplied to the reactions (**Fig. 4C and 4D**). Additionally, GST-TbnSMase degradative activity towards EPC was shown via HPTLC (**Fig. S5**). GST-TbnSMase was also incubated with a lipid substrate mixture containing equimolar concentrations of SM (d18:1/6:0, Avanti Polar Lipids product no.860582) and EPC (d17:1/12:0, Avanti Polar Lipids product no.860529). This competition assay indicated GST-TbnSMase lacks a sphingolipid substrate preference (**Fig. S6**). However, given the high levels of substrate turnover for both species, it is possible increasing the concentrations of both substrates may lead to a more marked preference for SM over EPC. Additionally, as EPC (d17:1/12:0) is the only pure EPC substrate commercially available, it is not possible to assess the impact of varying the sphingoid base and fatty acid composition on substrate turnover.

Currently, pure IPC lipid species are only available commercially through custom synthesis. GST-TbnSMase was shown to catabolise a custom synthesised NBD-conjugated IPC substrate (**Fig. S7**). However, the synthetic nature of this IPC substrate makes it difficult to draw conclusions regarding the physiological relevance of this activity. It is well established that the prevalent sphingolipid in procyclic form *T. brucei* is IPC (Richmond *et al.*, 2010). Therefore, a lipid extract from procyclic parasites was used to form a mixed micelle IPC substrate for GST-TbnSMase. Negative ion mode scans to detect inositol-containing lipids (precursors of m/z 241) were used to identify the IPC species present in the procyclic

T. brucei extract (**Fig. 5A**). Negative ion mode survey scans were then employed to search for ceramide chloride adducts $[M + Cl]^-$. Significant peaks corresponding to ceramide species were observed in the active GST-TbnSMase reaction (**Fig. 5B**), and were only observed at low levels in the heat-inactivated control (**Fig. 5C**, see also **Fig. S8**). Taken together, these results suggest GST-TbnSMase is also capable of catabolising natural IPC species to form ceramide and inositol-1-phosphate.

The ability of GST-TbnSMase to degrade SM, EPC and IPC indicates the enzyme does not distinguish between its sphingolipid substrates based upon headgroup identity. To further explore this finding, GST-TbnSMase was incubated with a ceramide-1-phosphate (d18:1/16:0) substrate (Avanti Polar Lipids product no. 860533). A ceramide (d18:1/16:0) chloride adduct $[M + Cl]^-$ was apparent in the lipid extract from the active GST-TbnSMase reaction (**Fig. 6A**), and was absent from the control (**Fig. 6B**). This result suggests lipid headgroups are not involved in GST-TbnSMase substrate recognition. However, GST-TbnSMase does not appear to degrade glycosphingolipids, as no apparent catabolism was observed upon incubating GST-TbnSMase with a mixture of galactosylceramide substrate species (Sigma product no. C4905) (data not shown). This indicates that although GST-TbnSMase does not require a headgroup for lipid substrate turnover, features of the headgroup can impede substrate catabolism. It was also observed that the enzyme cannot degrade S-1-P (d18:1, Avanti Polar Lipids product no. 860492), as the level of the substrate species remained unchanged in lipid extracts from an active GST-TbnSMase reaction and controls (data not shown). This finding indicates ceramide is a crucial component of GST-TbnSMase sphingolipid substrates.

Finally, GST-TbnSMase activity towards choline-containing phospholipids was reassessed. During previous research into TbnSMase, catabolic activity towards PC and *lyso*-PC lipid substrates could not be detected (Young and Smith, 2010). Re-assessing GST-TbnSMase activity towards PC (16:0/16:0) using ESI-MS/MS analysis failed to establish any substrate turnover (Avanti Polar Lipids product no. 850355) (data not shown). However, precursors of m/z 184 scans in positive ion mode revealed that GST-TbnSMase does turnover *lyso*-PC species (**Fig. 7**). There was a marked reduction in *lyso*-PCs (16:0) and (18:0) only in the presence of active GST-TbnSMase (**Fig. 7A**), relative to a PC (10:0/10:0) standard included in all *lyso*-PC reactions. This decrease did not occur in the control (**Fig. 7B**). Additionally,

the *lyso*-PC analogues miltefosine and edelfosine were previously shown to inhibit GST-TbnSMase (Young and Smith, 2010). This led to speculation that the previously observed inhibition of the enzyme's activity by *lyso*-PC analogues may be due to these compounds acting as competing substrates. Testing miltefosine as a potential substrate for GST-TbnSMase (5-50 nmoles) in the Amplex® UltraRed assay system did not produce any data to suggest this *lyso*-PC analogue is turned over by GST-TbnSMase (data not shown). This indicates *lyso*-PC analogues are not competitive substrates for GST-TbnSMase. However, the possibility remains that these compounds may be tightly bound to the enzyme's active site, preventing the ChoP release required for assay detection.

DISCUSSION

Sphingolipid metabolism in kinetoplastid parasites has long been established as a potential target for anti-parasitic drug development (Smith and Bütikofer, 2010; Mina and Denny, 2017). However, research has focused almost exclusively on the pathways involved in sphingolipid biosynthesis. Initial research into the nSMase found in *T. brucei* showed this enzyme has sphingolipid catabolic activity (Young and Smith, 2010). TbnSMase is the only currently identified *T. brucei* protein that displays this function. Unusually, the parasites appear to lack phospholipase D activity, which generally facilitates eukaryotic SM and PC catabolism. The substrate specificity of TbnSMase was examined to improve understanding of *T. brucei* sphingolipid catabolism and salvage.

TbnSMase is now known to turnover SM, EPC and IPC sphingolipid species. This is consistent with the established sphingolipid composition of *T. brucei* (Richmond *et al.*, 2010; Guan and Mäser, 2017): IPC predominates in procyclic parasites, whilst almost equal proportions of SM and EPC species are found in the bloodstream form (Guan and Mäser, 2017). In light of this knowledge, it may seem unsurprising that TbnSMase is active towards all three of these sphingolipid classes, only distinguished structurally by their headgroup (choline, ethanolamine and inositol). However, to our knowledge, this breadth of sphingolipid substrate specificity has not been documented previously for a lipid catabolic enzyme. It is possible that other sphingolipid degradative enzymes (especially those found in other kinetoplastids) share this ability but have not been tested. If this wide-ranging substrate specificity is not found in mammalian nSMase homologues, it may be possible to exploit these differences to create TbnSMase-specific substrate analogue inhibitors. The

TbnSMase activity reported here precludes the need for other sphingolipid degradative enzymes in the ER and rationalises the constitutive expression of this enzyme in both procyclic and bloodstream forms. However, no activity towards glycosphingolipids was observed, indicating phosphate groups may be an obligatory feature of TbnSMase substrates. It has been reported that *T. brucei* possess trace levels of glycosphingolipids, glucosylceramide species having been identified in several studies (Uemura *et al.*, 2006; Fridberg *et al.*, 2008; Richmond *et al.*, 2010). These could be endocytosed host glycosphingolipids, as no glycosphingolipid biosynthetic enzymes have been formally identified in *T. brucei* (Uemura *et al.*, 2006; Richmond *et al.*, 2010; Guan and Mäser, 2017). Only galactosylceramide species were tested as possible substrates for TbnSMase, thus it remains possible the enzyme is active towards other glycosphingolipids. Alternatively, another (other) unidentified enzyme(s) may be responsible for *T. brucei* glycosphingolipid catabolism, possibly within the lysosome.

ESI-MS/MS analysis indicates that TbnSMase preferentially catabolises SM species with specific fatty acid chain lengths. A more significant decrease in SM 42:1 (d18:1/24:0)/SM 42:2 (d18:1/24:1) occurred relative to SM 36:1 (d18:1/18:0), despite the latter species being more prevalent in the substrate mixture. This suggests that TbnSMase activity may be geared towards recycling specific long-chain fatty acids, which can then be utilised in other biosynthetic processes. Defining a crystal structure for TbnSMase may reinforce these preliminary observations, particularly if the structure provides insight into substrate binding and potential regulation. Few crystal structures for nSMase proteins are currently available, and most studies have focused on the binding of choline phosphate to the active site (Openshaw *et al.*, 2005; Ago *et al.*, 2006). However, TbnSMase does not seem to distinguish between its substrates based on headgroup identity, instead appearing to preferentially degrade substrates with specific fatty acids. This finding indicates that the fatty acid composition of lipid substrates may be of greater interest when considering enzyme-substrate interactions. In support of this view, TbnSMase was shown to actively degrade ceramide-1-phosphate, which lacks a polar alcohol headgroup entirely. However, the enzyme was unable to catabolise sphingosine-1-phosphate, indicating the presence of an amide bound fatty acid at the *sn*-2 position is vital for sphingolipid substrate recognition. Indeed, in the case of TbnSMase, the critical aspect of lipid substrate recognition appears to centre on the binding of the phosphate and fatty acid moieties to sphingosine or glycerol backbones. TbnSMase is now known to degrade *lyso*-PC in addition to sphingolipids. This aspect of

TbnSMase activity brings the enzyme in line with the nSMase found in *Plasmodium falciparum* parasites (PfnSMase) (Hanada *et al.*, 2002). Both PfnSMase and TbnSMase are inactive towards PC substrates, despite their ability to degrade *lyso*-PCs. This points to the diacylglycerol moiety of phospholipids impairing substrate binding to these SMase enzymes, and that removal of the fatty acid at the *sn*-2 position alleviates this inhibition. Thus, the requirements for glycerophospholipid recognition are the inverse of sphingophospholipid recognition.

TbnSMase is the first identified *T. brucei* enzyme shown to be capable of degrading *lyso*-PCs, which are believed to be a primary source of parasite choline during bloodstream infection (Bowes *et al.*, 1993; Smith and Bütikofer, 2010; Macêdo *et al.*, 2013). This is due to the parasites lacking a choline *de novo* biosynthesis pathway (Smith and Bütikofer, 2010), and *lyso*-PC concentration in the blood being 10-fold greater than choline (Macêdo *et al.*, 2013). Mammalian bloodstream *T. brucei* require an abundant source of choline, as over 50% of their lipid complement consists of choline-containing lipids (Smith and Bütikofer, 2010). The *T. brucei* phospholipase A₁ was shown to degrade PC, but not *lyso*-PC species (Richmond and Smith, 2007a; b). A plasma membrane phospholipase that degrades *lyso*-PC has been postulated (Bowes *et al.*, 1993) but has yet to be identified. This activity in TbnSMase indicates the enzyme may be responsible for *lyso*-PC turnover in the ER. Research into the essentiality of TbnSMase showed that compromised enzyme function led to a concomitant decrease in the parasite's rate of endocytosis (Young and Smith, 2010). This could have wide-ranging effects on the parasites, but was thought to have particularly impacted *T. brucei* choline homeostasis due to the parasites' dependence upon endocytosed and recycled choline-containing lipids. This impact was indicated by a marked decrease in phosphatidylcholine (PC) and increased intracellular diacylglycerol (DAG), suggesting PC *de novo* biosynthesis via the Kennedy pathway had been disrupted (Young and Smith, 2010). The newly discovered ability of TbnSMase to degrade *lyso*-PC and SM species aligns with these observations, indicating decreased enzyme activity has a direct impact on choline homeostasis. This underlines the importance of TbnSMase function in sustaining the intracellular choline metabolite levels required for parasite survival and propagation.

Further research is required to identify and characterise other enzymes that underpin lipid catabolism and salvage in these kinetoplastid parasites, which represent a valuable model

454 system for eukaryotic lipid metabolism (Serricchio and Bütikofer, 2011). As in the case of
455 TbnSMase, the activity of these enzymes may prove vital, opening new areas of *T. brucei*
456 biochemistry to drug development.

457 **ACKNOWLEDGEMENTS**

458 NBD-inositol-phosphoceramide (NBD-IPC) was kindly gifted by Dr. K. Zhang (Texas Tech
459 University).

460 **FINANCIAL SUPPORT**

461 This work was supported primarily through the European Community's Seventh Framework
462 Programme under grant agreements No. 602773 (Project KINDRED), with additional support
463 from Wellcome Trust Project grant (086658); Medical Research Council (MR/Mo20118/1)
464 and the School of Chemistry (The University of St Andrews).

465

REFERENCES

- Ago, H, Oda, M, Takahashi, M, Tsuge, H, Ochi, S, Katunuma, N, Miyano, M and Sakurai, J** (2006) Structural basis of the sphingomyelin phosphodiesterase activity in neutral sphingomyelinase from *Bacillus cereus*. *Journal of Biological Chemistry* **281**, 16157–67. doi: 10.1074/jbc.M601089200.
- Avanti Polar Lipids** (2018) 860062 Brain SM, Sphingomyelin (Brain, Porcine). Retrieved from Avanti Polar Lipids website: <https://avantilipids.com/product/860062> (accessed 24 January 2018)
- Bligh, EG, Dyer, WJ** (1959) A Rapid Method of total Lipid Extraction and Purification. *Canadian Journal of Biochemistry and Physiology* **37**, 911–917. doi: 10.1139/o59-099
- Bowes, E, Samad, H, Jiang, P, Weaver, B and Mellors, A** (1993) The acquisition of lysophosphatidylcholine by African trypanosomes. *Journal of Biological Chemistry* **268**, 13885–92.
- Brun, R and Schönenberger, M** (1979) Cultivation and in vitro cloning or procyclic culture forms of *Trypanosoma brucei* in a semi-defined medium. Short communication. *Acta Tropica* **36**, 289–292. doi: 10.5169/seals-312533.
- De Lederkremer, RM, Agusti, R and Docampo, R** (2011) Inositolphosphoceramide metabolism in *Trypanosoma cruzi* as compared with other trypanosomatids. *Journal of Eukaryotic Microbiology* **58**, 79–87. doi: 10.1111/j.1550-7408.2011.00533.x.
- Denny, PW, Goulding, D, Ferguson, MAJ and Smith, DF** (2004) Sphingolipid-free *Leishmania* are defective in membrane trafficking, differentiation and infectivity. *Molecular Microbiology* **52**, 313–27. doi: 10.1111/j.1365-2958.2003.03975.x.

- 490 **Denny, PW, Shams-Eldin, H, Price, HP, Smith, DF and Schwartz, RT** (2006) The
491 protozoan inositol phosphorylceramide synthase: a novel drug target which defines a new
492 class of sphingolipid synthase. *Journal of Biological Chemistry* **281**, 28200–28209. doi:
493 10.1074/jbc.M600796200
- 494 **Fridberg, A, Olson, CL, Nakayasu, ES, Tyler, KM, Almeida, IC and Engman, DM**
495 (2008) Sphingolipid synthesis is necessary for kinetoplast segregation and cytokinesis in
496 *Trypanosoma brucei*. *Journal of Cell Science* **121**, 522–35. doi: 10.1242/jcs.016741.
- 497 **Gerold, P and Schwarz, RT** (2001) Biosynthesis of glycosphingolipids de-novo by the
498 human malaria parasite *Plasmodium falciparum*. *Molecular and Biochemical*
499 *Parasitology* **112**, 29–37. doi: 10.1016/S0166-6851(00)00336-4.
- 500 **Goren, MA, Fox, BG and Bangs, JD** (2011) Amino acid determinants of substrate
501 selectivity in the *Trypanosoma brucei* sphingolipid synthase family. *Biochemistry* **50**,
502 8853–8861. doi: 10.1021/bi200981a.
- 503 **Guan, XL and Mäser, P** (2017) Comparative sphingolipidomics of disease-causing
504 trypanosomatids reveal unique lifecycle- and taxonomy-specific lipid chemistries.
505 *Scientific Reports* **7**, 1–13. doi: 10.1038/s41598-017-13931-x.
- 506 **Hanada, K, Palacpac, NMQ, Magistrado, PA, Kurokawa, K, Rai, G, Sakata, D, Hara,**
507 **T, Horii, T, Nishijima, M and Mitamura, T** (2002) *Plasmodium falciparum*
508 phospholipase C hydrolyzing sphingomyelin and lysocholinephospholipids is a possible
509 target for malaria chemotherapy. *Journal of Experimental Medicine* **195**, 23–34.
- 510 **Jenkins, RW, Canals, D and Hannun, YA** (2009) Roles and regulation of secretory and
511 lysosomal acid sphingomyelinase. *Cellular Signalling* **21**, 836–846. doi:
512 10.1016/j.cellsig.2009.01.026.
- 513

- 514 **Jenkins, RW, Idkowiak-Baldys, J, Simbari, F, Canals, D, Roddy, P, Riner, CD, Clarke,**
 515 **CJ and Hannun, YA** (2011) A novel mechanism of lysosomal acid sphingomyelinase
 516 maturation: requirement for carboxyl-terminal proteolytic processing. *Journal of*
 517 *Biological Chemistry* **286**, 3777–88. doi: 10.1074/jbc.M110.155234.
- 518 **Kolter, T and Sandhoff, K** (1999) Sphingolipids-Their Metabolic Pathways and the
 519 Pathobiochemistry of Neurodegenerative Diseases. *Angewandte Chemie (International*
 520 *ed. in English)* **38**, 1532–1568. doi: 10.1002/(SICI)1521-
 521 3773(19990601)38:11<1532::AID-ANIE1532>3.0.CO;2-U
- 522 **Macêdo, JP, Schmidt, RS, Mäser, P, Rentsch, D, Vial, HJ, Sigel, E and Bütikofer, P**
 523 (2013) Characterization of choline uptake in *Trypanosoma brucei* procyclic and
 524 bloodstream forms. *Molecular and Biochemical Parasitology* **190**, 16–22. doi:
 525 10.1016/j.molbiopara.2013.05.007.
- 526 **McConville, MJ and Naderer, T** (2011) Metabolic pathways required for the intracellular
 527 survival of *Leishmania*. *Annual Review of Microbiology* **65**, 543–61. doi:
 528 10.1146/annurev-micro-090110-102913.
- 529 **Mina, JGM and Denny, PW** (2017) Everybody needs sphingolipids, right! Mining for new
 530 drug targets in protozoan sphingolipid biosynthesis. *Parasitology* 1–14. doi:
 531 10.1017/S0031182017001081.
- 532 **Mina, JG, Pan, S-Y, Wansadhipathi, NK, Bruce, CR, Shams-Eldin, H, Schwarz, RT,**
 533 **Steel, PG and Denny, PW** (2009) The *Trypanosoma brucei* sphingolipid synthase, an
 534 essential enzyme and drug target. *Molecular and Biochemical Parasitology* **168**, 16–23.
 535 doi: 10.1016/j.molbiopara.2009.06.002.
- 536 **Mugnier, MR, Stebbins, CE and Papavasiliou, FN** (2016) Masters of Disguise: Antigenic
 537 Variation and the VSG Coat in *Trypanosoma brucei*. *PLoS Pathogens* **12**, 1–6. doi:
 538 10.1371/journal.ppat.1005784.

- 539 **Openshaw, AEA, Race, PR, Monzó, HJ, Vázquez-Boland, J-A and Banfield, MJ** (2005)
 540 Crystal structure of SmcL, a bacterial neutral sphingomyelinase C from *Listeria*.
 541 *Journal of Biological Chemistry* **280**, 35011–7. doi: 10.1074/jbc.M506800200.
- 542 **Richmond, GS and Smith, TK** (2007a) A novel phospholipase from *Trypanosoma brucei*.
 543 *Molecular Microbiology* **63**, 1078–1095. doi: 10.1111/j.1365-2958.2006.05582.x.A.
- 544 **Richmond, GS and Smith, TK** (2007b) The role and characterization of phospholipase A1
 545 in mediating lysophosphatidylcholine synthesis in *Trypanosoma brucei*. *Biochemical*
 546 *Journal* **405**, 319–29. doi: 10.1042/BJ20070193.
- 547 **Richmond, GS, Gibellini, F, Young, SA, Major, L, Denton, H, Lilley, A and Smith, TK**
 548 (2010) Lipidomic analysis of bloodstream and procyclic form *Trypanosoma brucei*.
 549 *Parasitology* **137**, 1357–92. doi: 10.1017/S0031182010000715.
- 550 **Serricchio, M and Bütikofer, P** (2011) *Trypanosoma brucei*: a model micro-organism to
 551 study eukaryotic phospholipid biosynthesis. *FEBS journal* **278**, 1035–46. doi:
 552 10.1111/j.1742-4658.2011.08012.x.
- 553 **Sevova, ES, Goren, MA, Schwartz, KJ, Hsu, F-F, Turk, J, Fox, BG and Bangs, JD**
 554 (2010) Cell-free synthesis and functional characterization of sphingolipid synthases
 555 from parasitic trypanosomatid protozoa. *Journal of Biological Chemistry* **285**, 20580–7.
 556 doi: 10.1074/jbc.M110.127662.
- 557 **Shaw, APM, Cecchi, G, Wint, GRW, Mattioli, RC and Robinson, TP** (2014) Mapping the
 558 economic benefits to livestock keepers from intervening against bovine trypanosomosis
 559 in Eastern Africa. *Preventive Veterinary Medicine* **113**, 197–210. doi:
 560 10.1016/j.prevetmed.2013.10.024.
- 561 **Smith, TK and Bütikofer, P** (2010) Lipid metabolism in *Trypanosoma brucei*. *Molecular*
 562 *and Biochemical Parasitology* **172**, 66–79. doi: 10.1016/j.molbiopara.2010.04.001.
- 563

- 564 **Sutterwala, SS, Hsu, F-F, Sevova, ES, Schwartz, KJ, Zhang, K, Key, P, Turk, J,**
 565 **Beverley, SM and Bangs, JD** (2008) Developmentally regulated sphingolipid synthesis
 566 in African trypanosomes. *Molecular Microbiology* **70**, 281–96. doi: 10.1111/j.1365-
 567 2958.2008.06393.x.
- 568 **Tidhar, R and Futerman, AH** (2013) The complexity of sphingolipid biosynthesis in the
 569 endoplasmic reticulum. *Biochimica et Biophysica Acta* **1833**, 2511–8. doi:
 570 10.1016/j.bbamcr.2013.04.010.
- 571 **Uemura, A, Watarai, S, Kushi, Y, Kasama, T, Ohnishi, Y and Kodama, H** (2006)
 572 Analysis of neutral glycosphingolipids from *Trypanosoma brucei*. *Veterinary*
 573 *Parasitology* **140**, 264–272. doi: 10.1016/j.vetpar.2006.04.028.
- 574 **Wirtz, E, Leal, S, Ochatt, C and Cross, GA** (1999) A tightly regulated inducible expression
 575 system for conditional gene knock-outs and dominant-negative genetics in *Trypanosoma*
 576 *brucei*. *Molecular and Biochemical Parasitology* **99**, 89–101.
- 577 **World Health Organization** (2017a) Trypanosomiasis, human African (sleeping sickness).
 578 Retrieved from the World Health Organization website:
 579 <http://www.who.int/mediacentre/factsheets/fs259/en/> (accessed 25 August 2017)
- 580 **World Health Organization** (2017b) *Integrating neglected tropical diseases into global*
 581 *health and development: fourth WHO report on neglected tropical diseases*. Geneva,
 582 Switzerland: World Health Organization.
- 583 **Xu, W, Xin, L, Soong, L and Zhang, K** (2011) Sphingolipid degradation by *Leishmania*
 584 major is required for its resistance to acidic pH in the mammalian host. *Infection and*
 585 *Immunity* **79**, 3377–87. doi: 10.1128/IAI.00037-11.
- 586 **Young, SA and Smith, TK** (2010) The essential neutral sphingomyelinase is involved in the
 587 trafficking of the variant surface glycoprotein in the bloodstream form of *Trypanosoma*
 588 *brucei*. *Molecular Microbiology* **76**, 1461–82. doi: 10.1111/j.1365-2958.2010.07151.x.

- Zhang, K, Pompey, JM, Hsu, F-F, Key, P, Bandhuvula, P, Saba, JD, Turk, J and Beverley, SM** (2007) Redirection of sphingolipid metabolism toward de novo synthesis of ethanolamine in *Leishmania*. *EMBO journal* **26**, 1094–104. doi: 10.1038/sj.emboj.7601565.
- Zhang, O, Wilson, MC, Xu, W, Hsu, F-F, Turk, J, Kuhlmann, FM, Wang, Y, Soong, L, Key, P, Beverley, SM and Zhang, K** (2009) Degradation of host sphingomyelin is essential for *Leishmania* virulence. *PLoS pathogens* **5**, e1000692. doi: 10.1371/journal.ppat.1000692.
- Zhang, O, Xu, W, Balakrishna Pillai, A and Zhang, K** (2012) Developmentally regulated sphingolipid degradation in *Leishmania major*. *PloS one* **7**, e31059. doi: 10.1371/journal.pone.0031059.

FIGURE LEGENDS

Fig. 1: *Trypanosoma brucei* sphingolipid metabolism. A) The currently proposed pathway for *T. brucei* *de novo* sphingolipid biosynthesis is shown. SPT-serine-palmitoyltransferase (Q580D0); 3-KSR – 3-ketosphinganine reductase (Q38BJ6); CerS – ceramide synthase (Q57V92, Q583F9); DES – dihydroceramide desaturase (Q583N4); TbSLSs 1-4 – *T. brucei* sphingolipid synthases 1-4 (Q38E53; Q38E54; Q38E55; Q38E56). Biosynthesis of ceramide (36:1) has been used here as an example. B) A simplified overview of eukaryotic sphingolipid degradation is provided (omitting glycosphingolipid catabolic pathways). A representative sphingolipid species (sphingomyelin (36:1)) is degraded in a step-wise process involving sphingomyelinases (SMases) and ceramidases (CDases). Lipid headgroups, such as choline phosphate, and sphingosine can be recycled to participate in *de novo* biosynthesis via the salvage pathway (green dashed arrows). Products ceramide and sphingosine can also be phosphorylated to produce signalling molecules ceramide-1-phosphate and sphingosine-1-phosphate respectively. ATP – adenosine triphosphate; ADP – adenosine diphosphate; CERK – ceramide kinase; SphK – sphingosine kinase.

Fig. 2: ESI-MS/MS analysis of sphingomyelin substrate reactions. Spectra are ESI-MS/MS precursor ion scans to detect choline-containing lipids (precursors of *m/z* 184) in positive ion mode. A) GST-TbnSMase-enriched bacterial membranes plus SM substrate. B) heat-inactivated GST-TbnSMase enriched bacterial membranes plus SM substrate. (†) Highlights the dimyristoyl-PC (28:0) standard (500 pmoles). C) Peak intensities (cps), normalised against the intensity of the dimyristoyl-PC (28:0) standard,

619 for each significant sphingomyelin (SM) substrate lipid species are depicted. Values are mean intensities for
 620 triplicate reactions ($n = 3$). Error bars represent the standard error of each mean (\pm).

621 **Fig. 3: GST-TbnSMase catabolism of sphingomyelin yields ceramide and choline phosphate.** Spectra are
 622 ESI-MS/MS survey scans in negative ion mode. A) GST-TbnSMase-enriched bacterial membranes plus SM
 623 substrate. B) heat-inactivated TbnSMase-enriched bacterial membranes plus SM substrate. Annotated ceramides
 624 have formed chloride adducts $[M + Cl]^-$. (*) Highlights previously identified significant contaminants of
 625 negative ion mode surveys thought to be associated with the detergent. C) Aqueous fractions of sphingomyelin
 626 substrate reactions were used as substrates for the Amplex® UltraRed assay system, plus (+) or minus (-) the
 627 coupling-enzyme alkaline phosphatase (AlkPhos). Change in fluorescence (millirelative-fluorescence units per
 628 minute (mrflu min^{-1})) was monitored spectrophotometrically. Values represent average rate of fluorescence
 629 change for aqueous fractions derived from triplicate reactions ($n = 3$). Error bars represent the standard error of
 630 each mean (\pm).

631 **Fig. 4: ESI-MS/MS analysis of ethanolamine-phosphoceramide substrate reactions.** Spectra are
 632 ESI-MS/MS survey scans in negative ion mode. A) EPC only (minus Triton X-100 detergent).
 633 B) GST-TbnSMase-enriched bacterial membranes plus EPC substrate. Annotated ceramides have formed
 634 chloride adducts $[M + Cl]^-$. C) heat-inactivated GST-TbnSMase-enriched bacterial membranes plus EPC
 635 substrate. D) EPC/ Triton X-100 detergent mixed micelle substrate only. (*) Highlights previously identified
 636 significant contaminants of negative ion mode surveys thought to be associated with the detergent.

637 **Fig. 5: ESI-MS/MS analysis of *T. brucei* procyclic-extract (inositol-phosphoceramide) substrate reactions.**
 638 A) ESI-MS/MS precursor ion scan of the procyclic lipid extract (IPC substrate) to detect inositol-containing
 639 lipids (precursors of m/z 241), in negative ion mode. The extract contains dihydroxylated ceramides, as well as
 640 trihydroxylated ceramides, the later denoted as 't-'. B) ESI-MS/MS negative ion mode survey scans were used to
 641 detect ceramides in GST-TbnSMase and C) heat-inactivated GST-TbnSMase-enriched bacterial membranes
 642 plus IPC substrate reactions. Annotated ceramides have formed chloride adducts $[M + Cl]^-$.

643 **Fig. 6: GST-TbnSMase catabolism of ceramide-1-phosphate yields ceramide.** Spectra are ESI-MS/MS
 644 survey scans in negative ion mode. A) GST-TbnSMase-enriched bacterial membranes plus
 645 ceramide-1-phosphate (C-1-P) substrate. B) Non-TbnSMase-expressing bacterial membranes plus
 646 ceramide-1-phosphate substrate. The annotated ceramide (Cer) product species has formed a
 647 chloride adduct $[M + Cl]^-$.

648 **Fig. 7: ESI-MS/MS analysis of lyso-PC substrate reactions.** Spectra are ESI-MS/MS precursor ion scans to
 649 detect choline-containing lipids (precursors of m/z 184) in positive ion mode. A) GST-TbnSMase-enriched
 650 bacterial membranes with lyso-PC substrate. B) non-TbnSMase-expressing bacterial membranes with lyso-PC
 651 substrate. (†) Highlights the didecanoyl-PC (20:0) standard (500 pmoles). (*) Highlights previously identified
 652 significant contaminants of positive ion mode scans thought to be associated with the detergent.

SUPPLEMENTARY MATERIAL

Full title: Investigating the Substrate Specificity of the Neutral Sphingomyelinase
from *Trypanosoma brucei*

Emily A. Dickie¹, Simon A. Young and Terry K. Smith

Biomedical Sciences Research Complex, Schools of Biology and Chemistry, University of St Andrews, Fife, KY169ST, UK

Running title: *T. brucei* neutral sphingomyelinase substrate specificity

Correspondence should be addressed to Terry K. Smith. Address: Biomedical Sciences Research Complex, Schools of Biology and Chemistry, University of St Andrews, Fife, KY169ST, UK. Telephone: +44(0)1334 463412. Email: tks1@st-andrews.ac.uk

¹ Current address: Wellcome Trust Centre for Molecular Parasitology, Institute of Infection, Immunity and Inflammation, College of Medical, Veterinary and Life Sciences, University of Glasgow, Glasgow, G12 8TA, UK

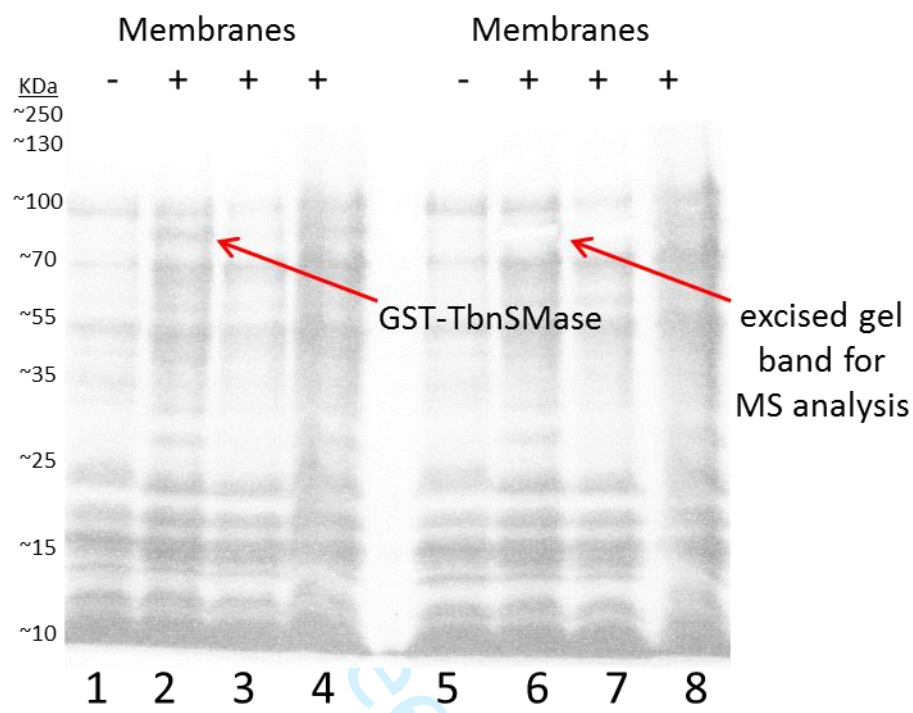


Fig. S1: Presence of GST-TbnSMase in bacterial membranes was confirmed by mass spectrometry analysis. pLysSGold *E. coli* membrane fractions were separated via SDS-PAGE and stained with Coomassie. Fractions were run in duplicate (lanes 1-4 and again, in lanes 5-8). ‘-’ indicates the non-TbnSMase-expressing control bacterial membranes. ‘+’ signifies membrane fractions were derived from *E. coli* expressing GST-TbnSMase. The band thought to correspond to GST-TbnSMase (annotated, lane 2) was excised (annotated, lane 6) and submitted for mass spectrometry analysis, which confirmed its identity as GST-TbnSMase.

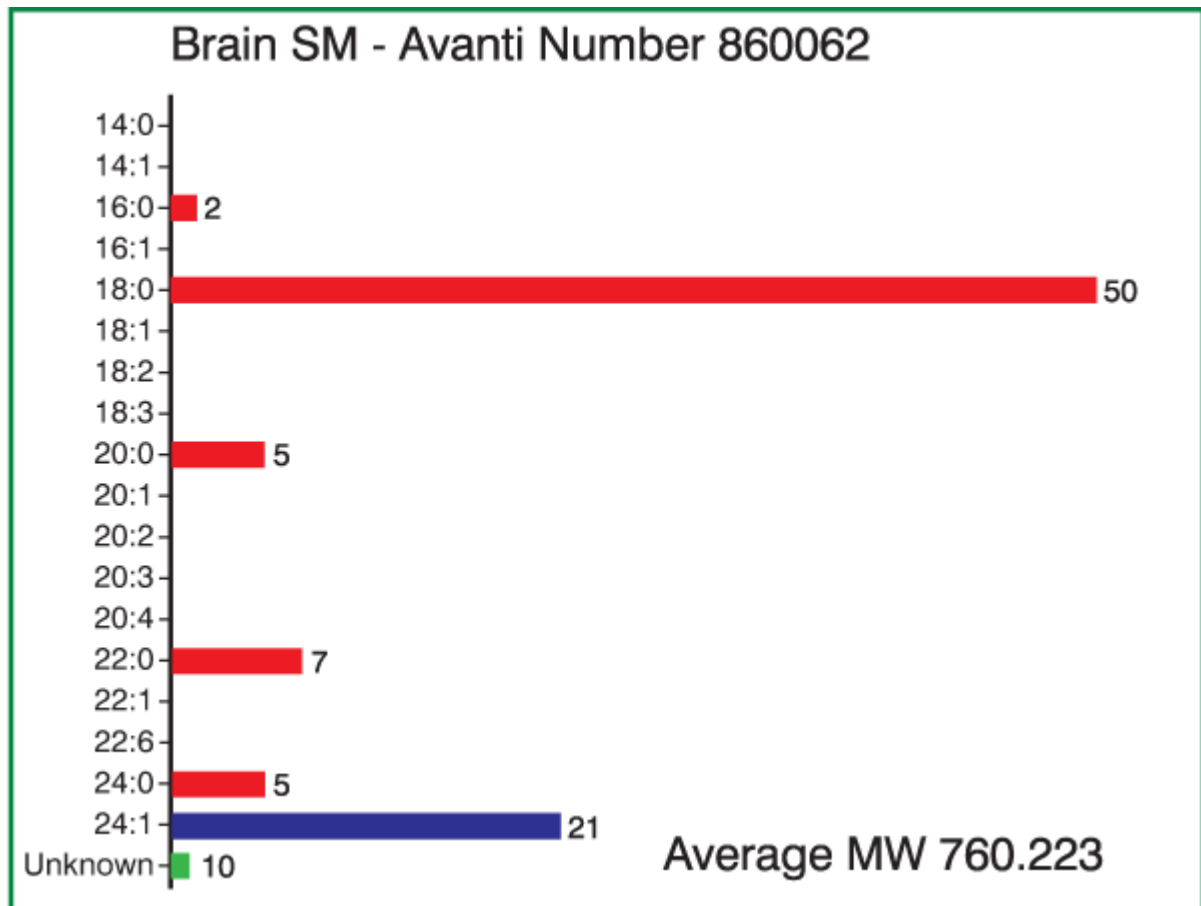


Fig S2: Avanti fatty acid analysis of brain SM product 860062. This product (<https://avantilipids.com/product/860062>) was used as an SM substrate for GST-TbnSMase (see **Fig. 2** and **Fig. S3**). Average fatty acid distribution for SM (d18:1/y) lipid species within the product are shown.

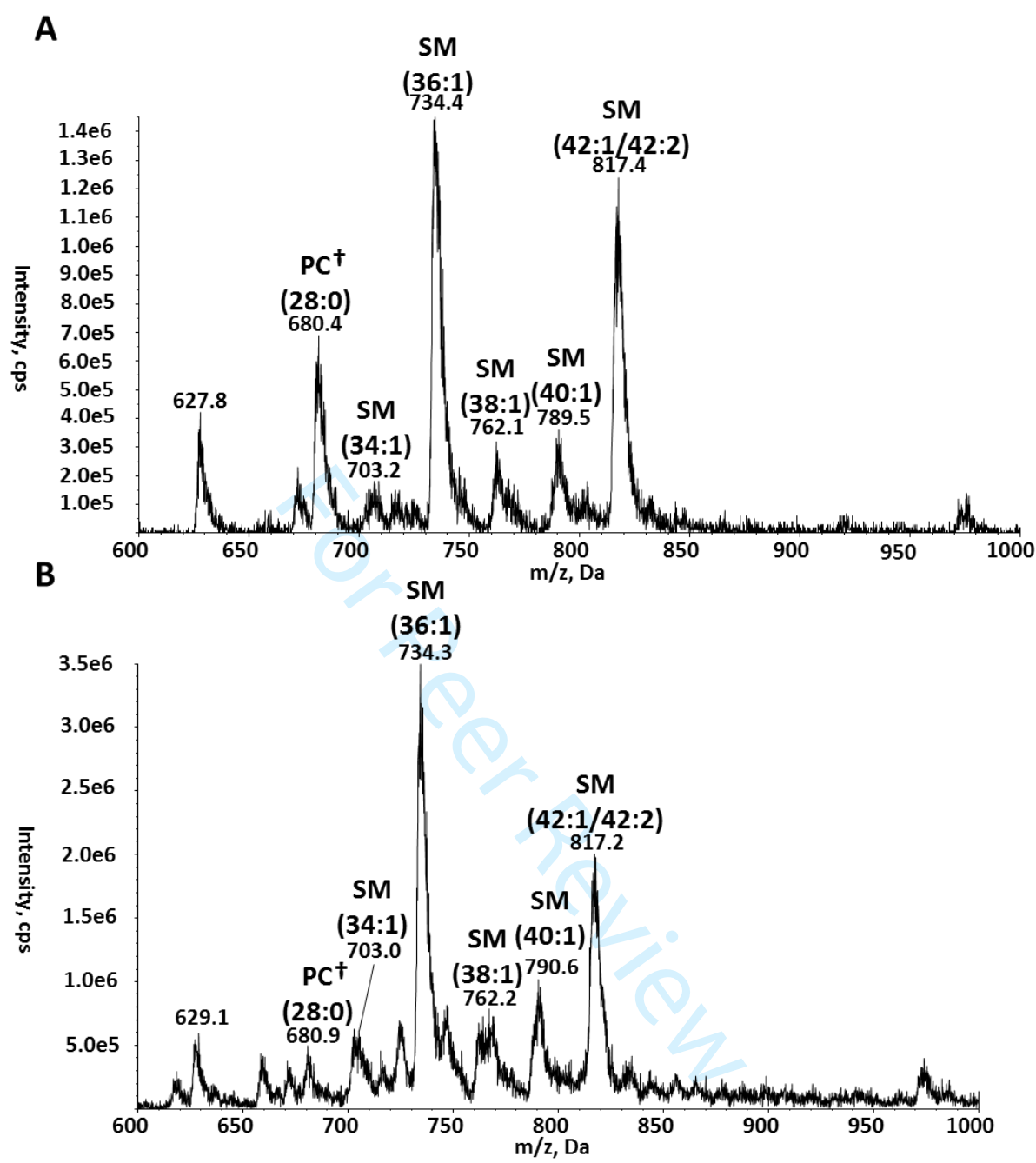


Fig. S3: Additional supporting spectra for GST-TbnSMase catabolism of sphingomyelin. Spectra are ESI-MS/MS precursor ion scans to detect choline-containing lipids (precursors of m/z 184) in positive ion mode. A) SM/Triton X-100 mixed micelle substrate only. B) Non-TbnSMase-expressing bacterial membranes plus SM substrate. (†) Highlights the dimyristoyl-PC (28:0) standard (500 pmoles).

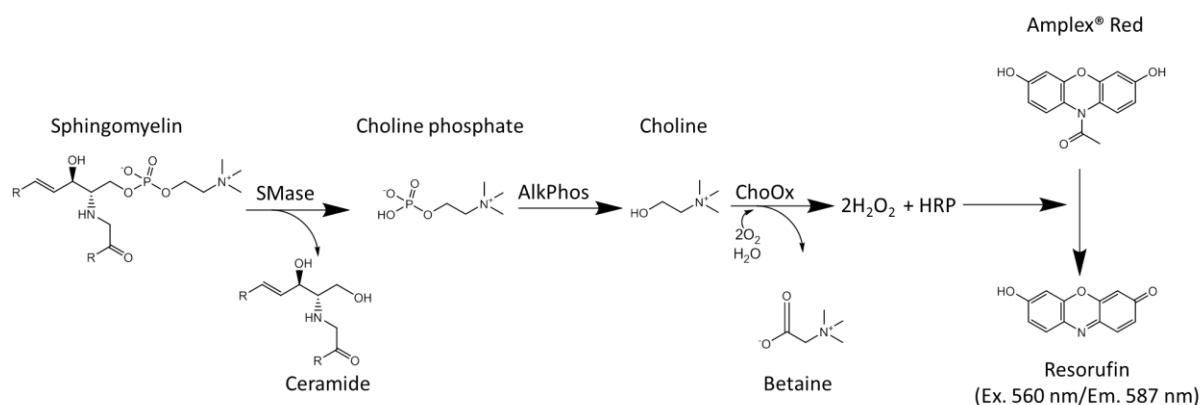


Fig. S4: Amplex® Red assay system. Sphingomyelinase (SMase) activity results in sphingomyelin substrate catabolism, producing ceramide and choline-phosphate (ChoP). ChoP is then hydrolysed by the assay coupling enzyme alkaline phosphatase (AlkPhos), forming choline (Cho). Choline oxidase (ChoOx) oxidises choline to yield betaine and hydrogen peroxide (H₂O₂). As the ChoOx used in the assay is isolated from *Alcaligenes sp.*, Cho is fully oxidised to betaine, via a betaine-aldehyde intermediate (not shown), and 2 moles of hydrogen peroxide (H₂O₂) are produced for every mole of Cho. The H₂O₂ is the oxidising agent for horseradish peroxidase (HRP) that catalyses the conversion of Amplex® Red to red-fluorescent resorufin. The rate of this conversion can be monitored spectrophotometrically (Ex. 560 nm, Em. 587 nm). For the work described here, Amplex® UltraRed, an optimised version of Amplex® Red, was used. However, no chemical structure or formula is available for Amplex® UltraRed and its red-fluorescent conversion product.

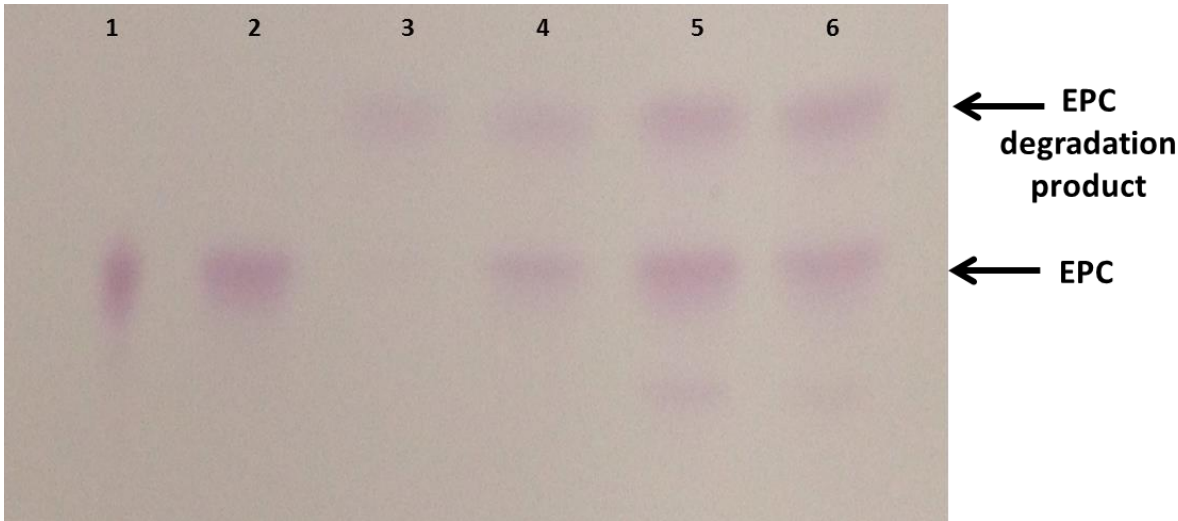


Fig. S5: HPTLC analysis of ethanolamine-phosphoceramide substrate reactions.

1) EPC stock solution (no Triton X-100 detergent); 2) EPC/Triton X-100 detergent mixed micelle substrate in reaction buffer; 3) GST-TbnSMase-enriched bacterial membranes plus EPC substrate; 4) non-TbnSMase-expressing bacterial membranes plus EPC substrate; 5) heat-inactivated GST-TbnSMase-enriched bacterial membranes plus EPC substrate; 6) heat-inactivated non-TbnSMase-expressing bacterial membranes plus EPC substrate.

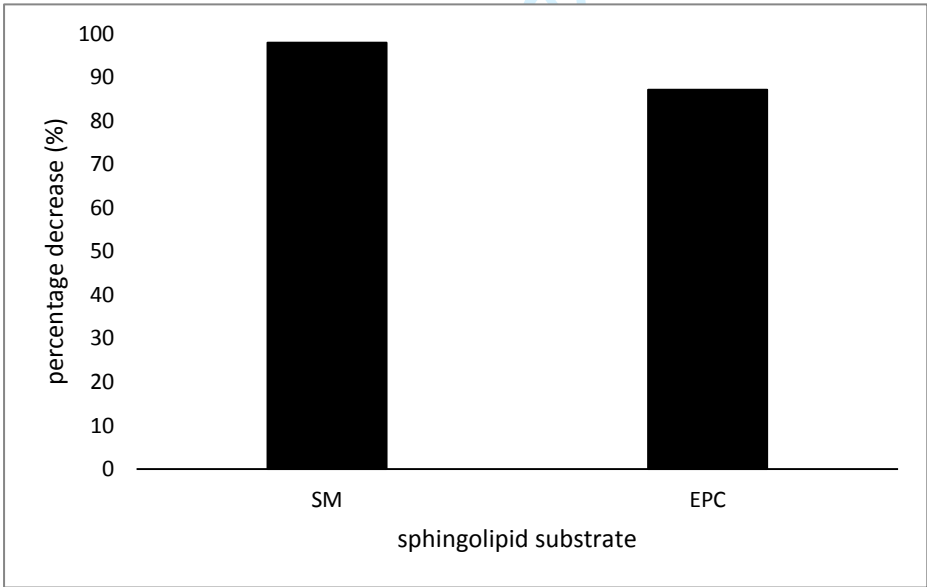


Fig. S6: Sphingomyelin and ethanolamine-phosphoceramide substrate competition assay. A substrate mixture, containing equimolar concentrations (25 nmoles) of sphingomyelin and ethanolamine-phosphoceramide, was incubated with GST-TbnSMase. The percentage decreases (%) in the level of each substrate, relative to a TbnSMase negative control, are shown.

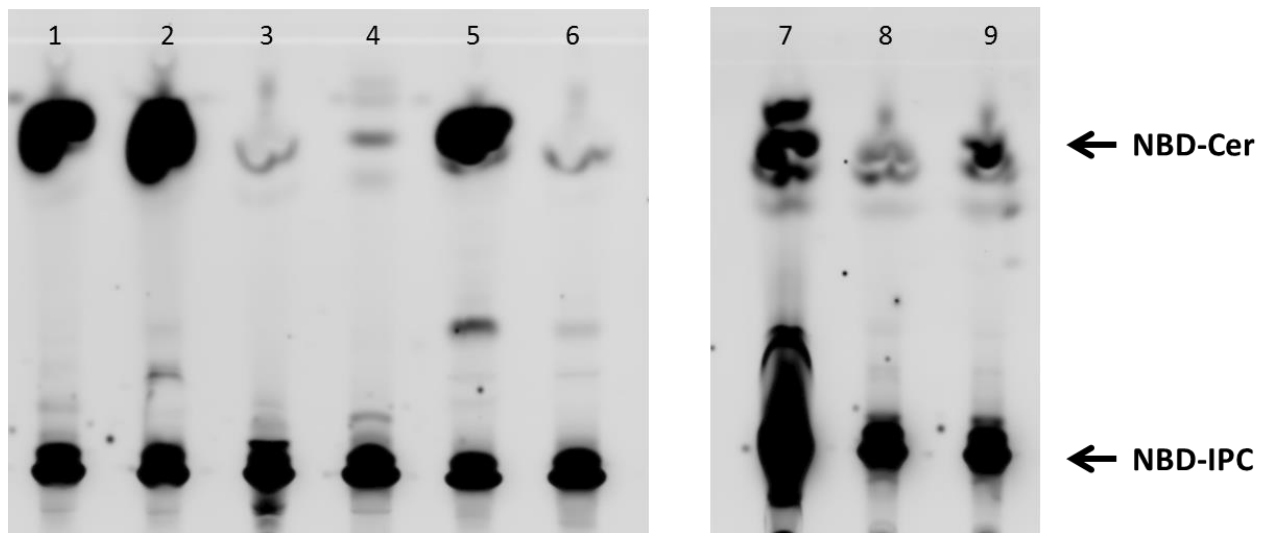


Fig. S7: HPTLC analysis of NBD-IPC substrate reactions. 1) bloodstream form *T. brucei* lysate with NBD-IPC substrate; 2) stumpy form *T. brucei* lysate with NBD-IPC substrate; 3) procyclic form *T. brucei* lysate with NBD-IPC substrate (stored prior to use); 4) NBD-IPC substrate only; 5) GST-TbnSMase-expressing *E. coli* lysate with NBD-IPC substrate; 6) non-GST-TbnSMase-expressing *E. coli* lysate with NBD-IPC substrate; 7) procyclic form *T. brucei* lysate with NBD-IPC substrate (freshly prepared); 8) promastigote form *L. major* lysate with NBD-IPC substrate; 9) epimastigote form *T. cruzi* lysate with NBD-IPC substrate.

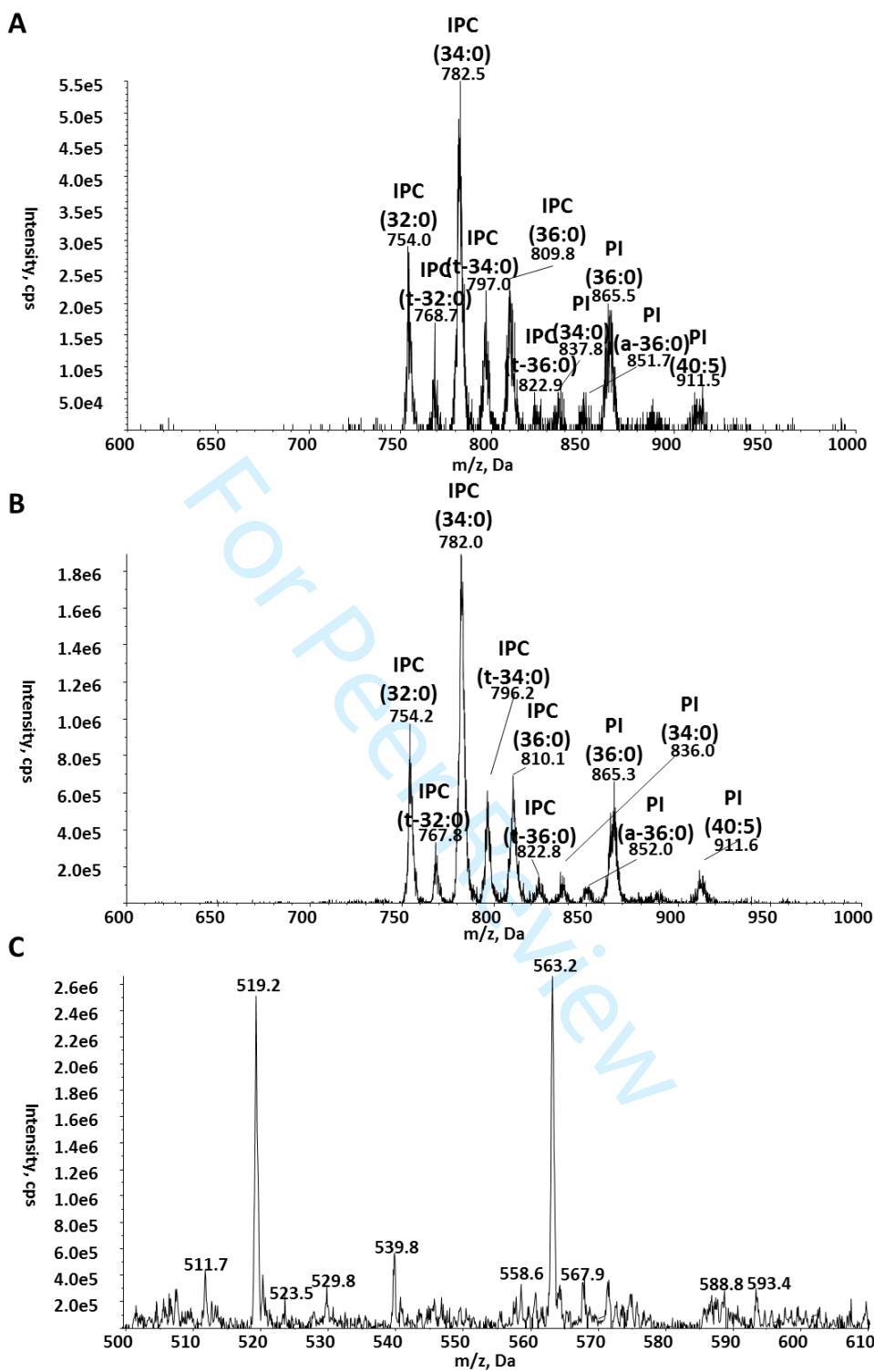


Fig. S8: Additional supporting spectra for *T. brucei* procyclic-extract (inositol-phosphoceramide) reactions. ESI-MS/MS precursor ion scans to detect inositol-containing lipids (precursors of m/z 241) in negative ion mode. A) GST-TbnSMase-enriched bacterial membranes plus procyclic extract (IPC) substrate. B) heat-inactivated GST-TbnSMase-enriched bacterial membranes plus IPC substrate. The substrate contains dihydroxylated ceramides, as well as trihydroxylated ceramides, the later denoted as 't-'. C) ESI-MS/MS survey scan, in negative ion mode, of the IPC/Triton X-100 detergent mixed micelle substrate only.

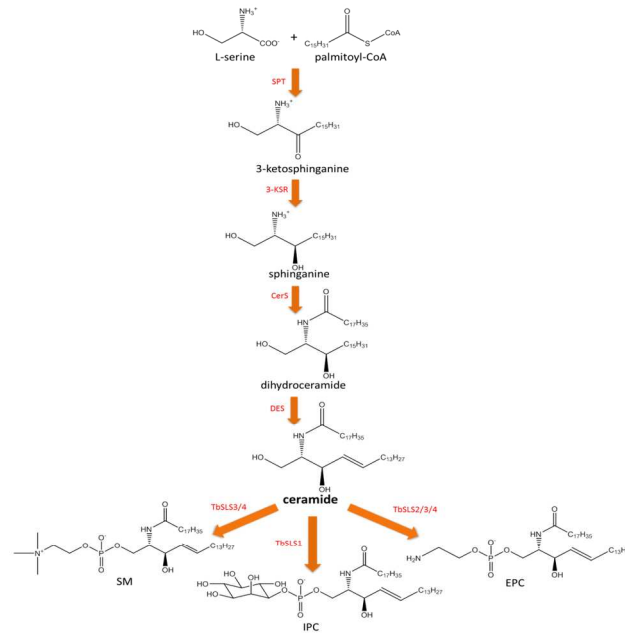
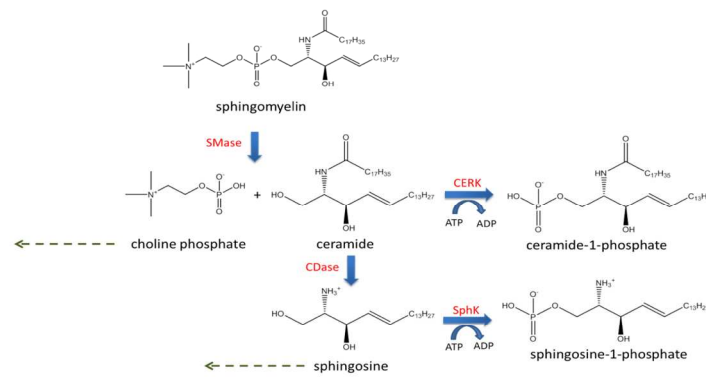
A**B**

FIG 1

190x275mm (192 x 192 DPI)

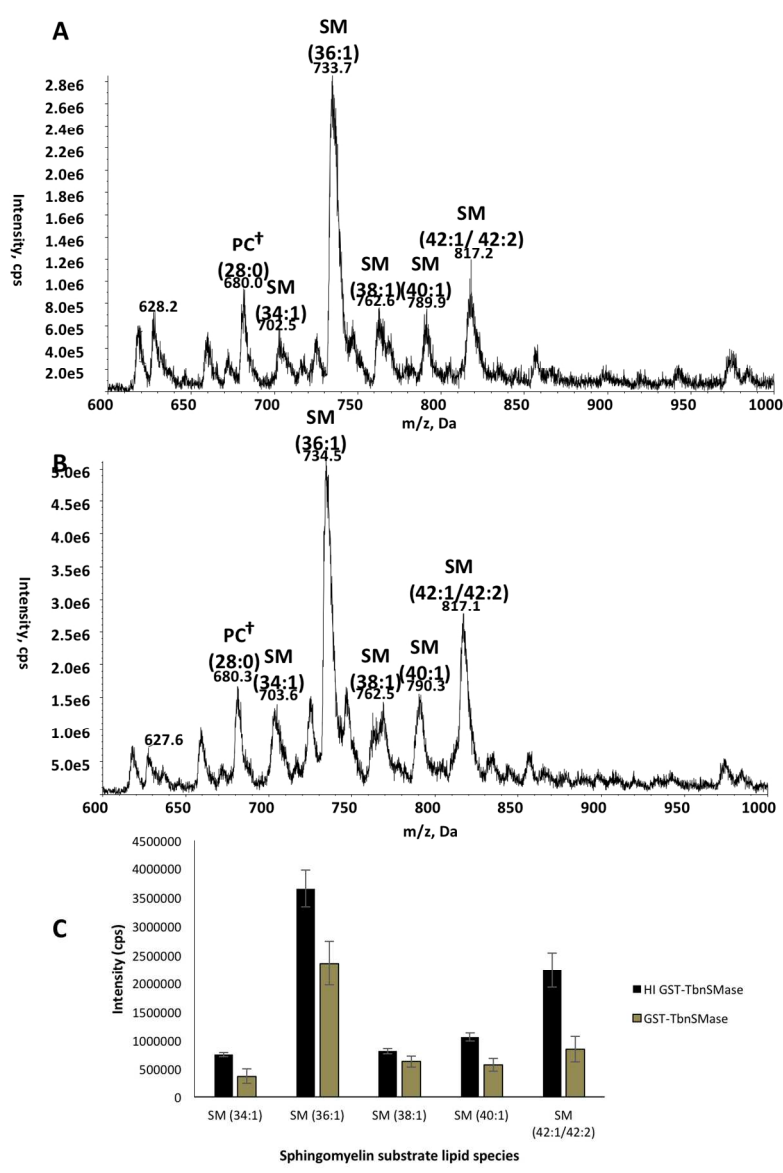


FIG 2

190x275mm (192 x 192 DPI)

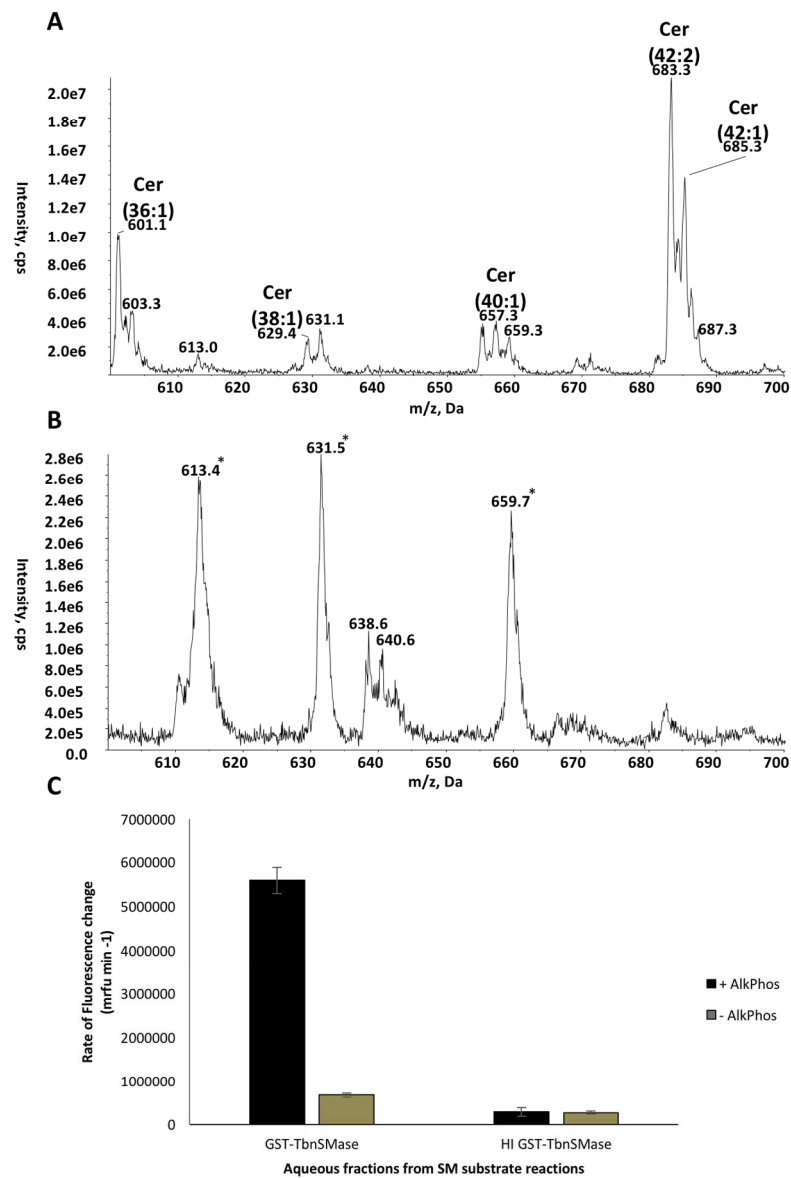


FIG 3

190x275mm (192 x 192 DPI)

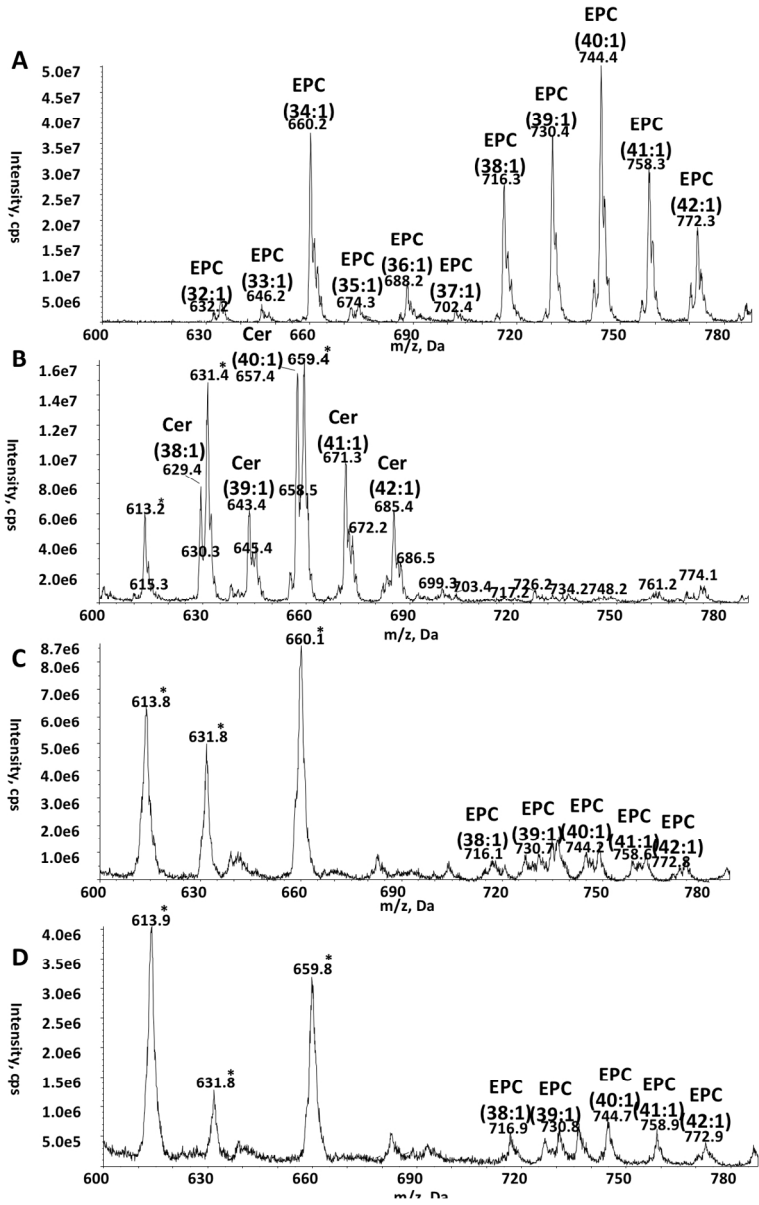


FIG 4

190x275mm (192 x 192 DPI)

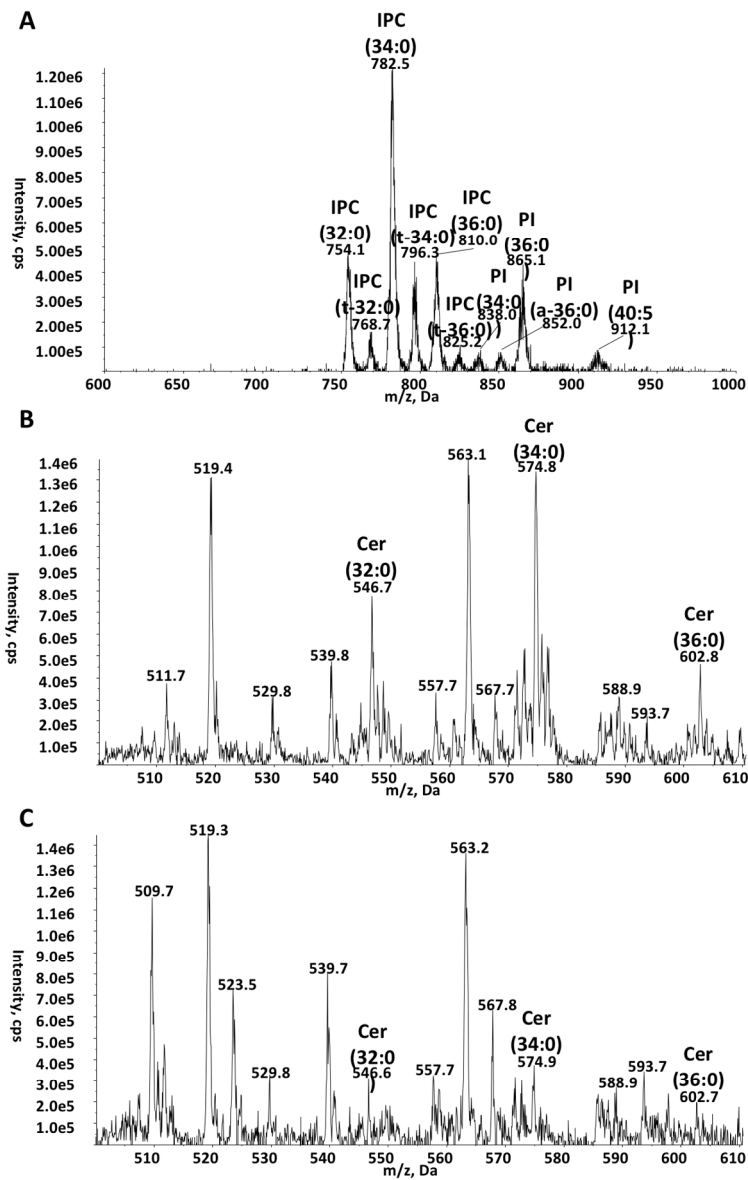


FIG 5

190x275mm (192 x 192 DPI)

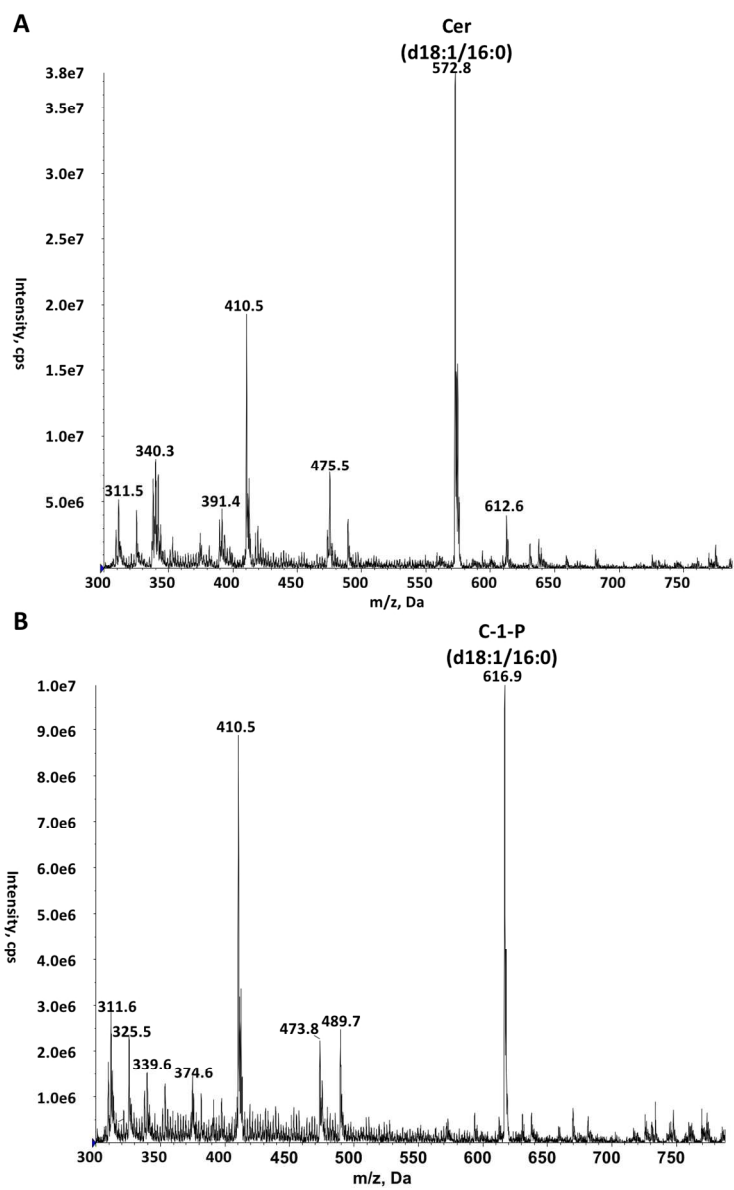


fig 6

190x275mm (192 x 192 DPI)

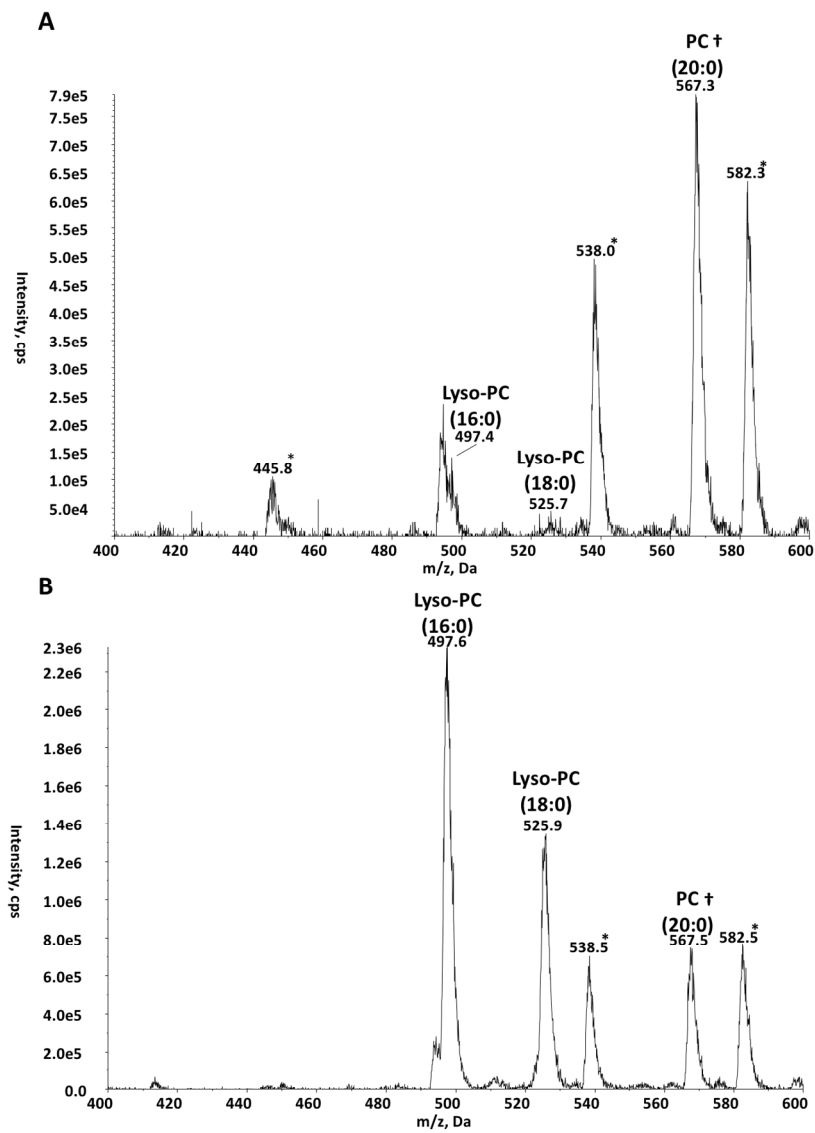


fig 7

190x275mm (192 x 192 DPI)